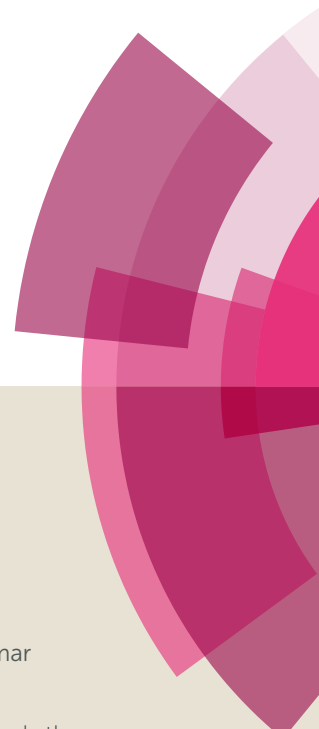


NJC

Accepted Manuscript



This article can be cited before page numbers have been issued, to do this please use: *. Shaily, A. Kumar and N. Ahmed, *New J. Chem.*, 2017, DOI: 10.1039/C7NJ02569F.



This is an Accepted Manuscript, which has been through the Royal Society of Chemistry peer review process and has been accepted for publication.

Accepted Manuscripts are published online shortly after acceptance, before technical editing, formatting and proof reading. Using this free service, authors can make their results available to the community, in citable form, before we publish the edited article. We will replace this Accepted Manuscript with the edited and formatted Advance Article as soon as it is available.

You can find more information about Accepted Manuscripts in the [author guidelines](#).

Please note that technical editing may introduce minor changes to the text and/or graphics, which may alter content. The journal's standard [Terms & Conditions](#) and the ethical guidelines, outlined in our [author and reviewer resource centre](#), still apply. In no event shall the Royal Society of Chemistry be held responsible for any errors or omissions in this Accepted Manuscript or any consequences arising from the use of any information it contains.



Journal Name

ARTICLE

Coumarin-chalcone hybrid as selective and sensitive colorimetric and turn-on fluorometric sensor for Cd²⁺ detection

Shaily^{*a,b}, Ajay Kumar and Naseem Ahmed^{*a}

Received 00th January 20xx,
Accepted 00th January 20xx

DOI: 10.1039/x0xx00000x

www.rsc.org/

Chalcone based Naked-Eye colorimetric chemical sensor (*E*)-4-hydroxy-3-(3-(4-methoxyphenyl)acryloyl)-2*H*-chromen-2-one **1a** was developed for selective and sensitive recognition of Cd²⁺ in mixed aqueous-organic media. The chemosensor demonstrate a distinct color change as well as remarkable variations in absorption and fluorescence enhancement in emission spectra upon interaction with Cd²⁺. The dual colorimetric and fluorometric responses of the chemosensor **1a** towards Cd²⁺ are attributed to the formation of a 1:1 [**1a**+Cd²⁺] complex, which eventually affects its optical properties. The association constant for Cd²⁺ towards receptor **1a** obtained from Benesi–Hildebrand plot and non-linear least square fitting were found to be $9.56 \times 10^5 \text{ M}^{-1}$ and $(1.34 \pm 0.87) \times 10^6 \text{ M}^{-1}$ respectively with a detection limit $5.84 \times 10^{-8} \text{ M}$. The fluorescence enhancement of chemosensor **1a** upon interaction with Cd²⁺ was attributed to chelation-enhanced fluorescence (CHEF) occurred at pH 7.0.

Introduction,

In recent years, the conservation, protection of water resources and contaminant prevention as well as anthropogenic activity is a challenging task for researchers and scientists.¹ Among various inorganic contaminants, the metal cations play a significant role as components of electrolytes and may also present inherent risks due to their potential impact on environment and human health.² A large range of metal ions are beneficial to the human health but some heavy metal ions such as Pb²⁺, Cd²⁺ and Hg²⁺ etc are toxic even in the presence of trace amounts. Considering the Pb²⁺, Cd²⁺ and Hg²⁺ ions as hazardous, the European Union's Restriction on Hazardous Substances directive banned the use of these ions in electrical and electronic equipments.³ Owing to the non-biodegradable nature, these metal ions accumulate in the environment leading to the contaminated food and water.⁴ Among the various transition metals cadmium is a silver-white soft metal that is naturally found at low levels in soil, rocks and small amounts in the earth's crust. Additionally, cadmium is widely used threshold limit value of 0.05 mg/m³ for cadmium salts and cadmium dust has been suggested in various fields such as agriculture, industry, alloys, metallurgy, electroplating, coloring matters and fertilizers as well as in the construction of dry-cell batteries.⁵ In spite of numerous uses and applications, cadmium is highly toxic and possess a severe threat to the health of human beings and environment. A major exposure

source of cadmium is smoking and for non-smokers the main source is food, but breathing in cadmium-containing dust is the most harmful route. Since the human body has no machinery to excrete Cd²⁺, it accumulates in tissues resulting in carcinogenic effects or physiological disorders and can cause serious injury to the human kidney, lung, bone and nervous system.⁶ Moreover, the epidemiological studies carried out on the populations of general human revealed that Cd²⁺ increase the threat of developing prostate, breast and endometrial cancers.⁷ According to the USA Act of Comprehensive Environmental Response, Liability and Compensation, cadmium is ranked 7th position in the merit of the top 275 Hazardous.^{8,9} According to United State Environmental Protection Agency (EPA) and WHO (World Health Organization) the maximum permissible limit of Cd²⁺ in drinking water is 5 µg/L and 3 µg/L respectively.^{10,11} In recent times, severe health problems and environmental pollution caused by Cd²⁺ make it in great demand for the development of methods to monitor and detect cadmium levels both in the environment and biological samples even at very low concentrations.¹²⁻¹⁴

Compared with traditional analytical techniques including voltammetric methods, inductively coupled plasma mass spectrometry (ICP-MS), ion selective electrodes and atomic absorption/emission spectrometry, the development of highly selective colorimetric/fluorescent chemosensors for recognition and sensing of environmentally and biologically significant metal ions has attracted significant attention due to their good selectivity, high sensitivity, simplicity and rapid response time.¹⁵⁻²⁰ These traditional analytical techniques generally suffer from several limitations such as laborious sample pretreatment processes, expensive instrumentations, specialized personnel and inadaptability for *in site* measurement. A plethora of various synthetic sensors

^a Department of Chemistry, Indian Institute of Technology, Roorkee-247667, India.

^b Department of Chemistry, D.B.S. (P.G.) College Dehradun-248001, India.

* Footnotes relating to the title and/or authors should appear here.

Electronic Supplementary Information (ESI) available: [details of any supplementary information available should be included here]. See DOI: 10.1039/x0xx00000x

ARTICLE

Journal Name

demonstrating fluorescent response toward Cd^{2+} have been reported in literature.²¹⁻³¹ As Zn^{2+} and Cd^{2+} have very similar chemical properties, many of these synthetic sensors can also respond to Zn^{2+} . In 2012, Liu *et al.* developed a highly selective quinoline based fluorescent sensor for Zn^{2+} and Cd^{2+} . Upon interaction with Cd^{2+} , sensor display a bright “switch-on” status based on the PET mechanism and with Zn^{2+} , demonstrate a distinct red shift in emission band based on the ICT mechanism with small emission enhancements.³² Hence, it has been an indispensable task great challenge for analysts to design and develop a Cd^{2+} selective fluorescence sensor.

There are several reports on the detection of cadmium ions using different probes.³³⁻³⁹ Normally, their sensing mechanism is based on the fluorescence quenching process (“turn-off”). In our fluorescence enhancement (“turn-on”) by complexation with heavy transition metal ions is highly desirable extended efforts to design and develop new metal ion and anion sensor with interesting structures feature and advanced functions,⁴⁰⁻⁴² herein we developed a novel discovery coumarin-chalcone hybrid fluorescent sensor, (*E*)-4-hydroxy-3-(3-(4-methoxyphenyl)acryloyl)-2*H*-chromen-2-one, **1a** fluorescence “turn-on” chemosensor for detecting cadmium ions which shows excellent selectivity and sensitivity towards Cd^{2+} over many other metal ions.

Results and discussion,

The synthesis of **1a** is outlined in Scheme 1. The chemical structures of the intermediates and final products were fully characterized by ¹H-NMR, ¹³C-NMR, FTIR spectroscopies, HRMS and UV-vis, spectra and all data are provided in the supporting information. The photophysical properties of **1a** were investigated by absorption and emission studies.

Colorimetric and Fluorimetric Responses of **1a** to Cd^{2+} ion

The synthesized chemosensor **1a** possess a conjugated β -hydroxy enone unit, which could coordinate with metal ion, and a coumarin moiety as a signaling unit. The optical properties and sensing behavior of chemosensor **1a** towards metal ions was studied through absorption and emission spectroscopy at room temperature in HEPES-buffered solution (20 mM, $\text{CH}_3\text{CN}:\text{H}_2\text{O}$, 3:7, v/v, pH 7.0). As shown in Figure 1a, upon addition of 10 equivalents of different metal ion (Na^+ , K^+ , Ba^{2+} , Ca^{2+} , Mg^{2+} , Cr^{3+} , Mn^{2+} , Fe^{3+} , Co^{2+} , Ni^{2+} , Cu^{2+} , Zn^{2+} , Pb^{2+} , Ag^+ , Al^{3+} , Cd^{2+} , Hg^{2+} , Hg^+ and Sn^{2+}) into the solution of **1a** (10 μM), an immediate and obvious change in color was observed from yellow to colorless only with Cd^{2+} . The results indicated that **1a** can act as a highly sensitive “naked-eye” sensor for Cd^{2+} ion. The absorption spectrum of **1a** represents a maxima centred at 387 nm, which may be attributed to the $\pi-\pi^*$ transitions of the coumarin motif. To gain an insight into the binding feature of **1a** toward Cd^{2+} , the UV-vis spectral changes upon the addition of different metal ions (10.0 equivalents) to the solution of **1a** were investigated. Fascinatingly, a new absorption maximum appears at 370 nm while the absorption band at 387 nm was completely disappeared only on

treatment of Cd^{2+} to **1a** solution (Figure 2). Thus, the chemosensor **1a** exhibited high selectivity and sensitivity for Cd^{2+} over other metal ions.

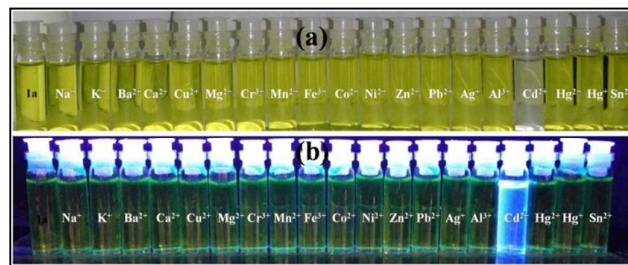


Figure 1: (a) Colorimetric. (b) Fluorometric changes after the addition of 10 equivalents of different metal ions to the solution of **1a** (10 μM) in HEPES-buffered solution (20 mM, $\text{CH}_3\text{CN}:\text{H}_2\text{O}$, 3:7, v/v, pH 7.0).

To further explore the interaction between **1a** and Cd^{2+} , UV-vis absorption titration of **1a** (10 μM) solution was monitored with different concentrations of Cd^{2+} (0–10 equivalents) in HEPES-buffered solution (20 mM, $\text{CH}_3\text{CN}:\text{H}_2\text{O}$, 3:7, v/v, pH 7.0). As shown in Figure 3, upon the gradual addition of Cd^{2+} (0–10 equivalents) to **1a** (10 μM) solution, the absorption band at 387 nm decreased slowly and gradually blue shifted with the generation of a new absorption band appeared at 370 nm. Thus the absorption spectrum became stable after the addition of 10 equivalents of Cd^{2+} to **1a** solution and no appreciable changes were observed on further addition of Cd^{2+} . These result suggested that a new species was produced during the titration. The metal complexation with **1a** may be due to its 4-hydroxycoumarin unit, leaving the enolic moiety, and chalcone moiety providing α,β -unsaturated carbonyl fraction available for metal complexation *via* the formation of one or even two coordination spheres. Thus leads to the formation of stable **1a**- Cd^{2+} complex. In order to find out the binding stoichiometry between **1a** and Cd^{2+} , the continuous variation method (Job’s plot) was used.⁴³ The total concentration of **1a** and Cd^{2+} was constant (10 μM), with a continuous variable molar fraction. The Job’s plot of **1a** with Cd^{2+} showed maxima at a mole fraction of 0.5, revealed that the complex formed between Cd^{2+} and **1a** follows a 1:1 binding stoichiometry (Figure S7 in the supporting information). In addition, the 1:1 complex formation between **1a** and Cd^{2+} was further supported by Benesi–Hildebrand plot providing a good linear relationship between the absorbance versus concentration of Cd^{2+} . The association constant of the **1a**- Cd^{2+} complex was then calculated to be $1.79 \times 10^6 \text{ M}^{-1}$ with a linear relationship by Benesi–Hildebrand plot as evident in inset (b) of Figure 3.⁴⁴ The association constant of the **1a** with Cd^{2+} was also evaluated by a non linear least-square fit of the absorbance vs the concentration of Cd^{2+} ion and found to be $(6.93 \pm 2.95) \times 10^5 \text{ M}^{-1}$ with good non linear relationship (Inset (a) of Figure 3)^{45, 46}.

The detection limit of chemosensor **1a** for Cd^{2+} analysis was determined from a plot of normalized absorbance as a function of the concentration of the added metal ions and

evaluated to be 6.309×10^{-8} M (Figure S8 in the supporting information).^{47, 48} The individual UV-vis absorbance response of **1a** against different metal ions revealed a remarkable selectivity towards Cd^{2+} (Figure 2).

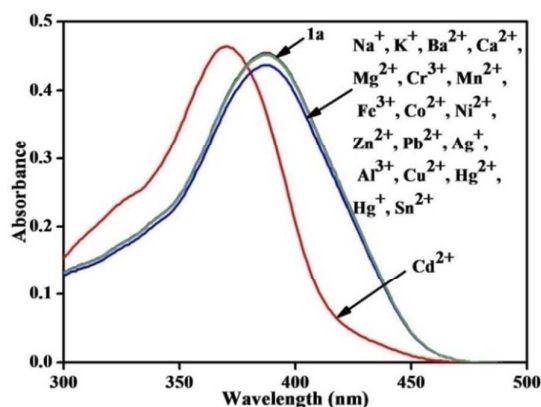


Figure 2: Absorption spectra of **1a** (10 μM) in presence of different metal ions in HEPES-buffered solution (20 mM, $\text{CH}_3\text{CN}:\text{H}_2\text{O}$, 3:7, v/v, pH 7.0).

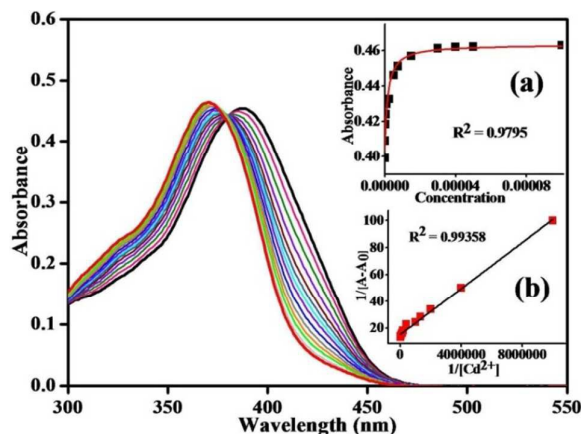


Figure 3: Absorption spectra of **1a** (10 μM) upon titration with Cd^{2+} (0–10 equiv) in HEPES-buffered solution (20 mM, $\text{CH}_3\text{CN}:\text{H}_2\text{O}$, 3:7, v/v, pH 7.0). Inset (a): Non linear fitting of absorbance data of **1a** with Cd^{2+} . and Inset (b) A good linear fit of Benesi-Hildebrand plot confirms the 1:1 binding stoichiometry.

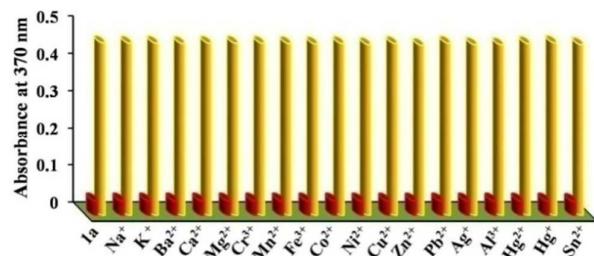
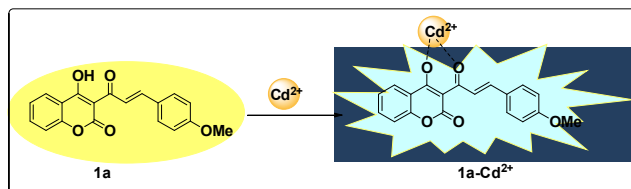


Figure 4: Metal-ion selectivity profiles of **1a** (10 μM) in HEPES-buffered solution (20 mM, $\text{CH}_3\text{CN}:\text{H}_2\text{O}$, 3:7, v/v, pH 7.0). Red bars represent the absorbance of **1a** in the presence of 10 equiv. of various metal ions. Yellow bars represent the absorbance of **1a**- Cd^{2+} complex in the presence of 10 equiv. of the indicated metal ions.

However, the most significant criterion for a metal ion selective chemosensor is the ability to sense a specific metal ion in the vicinity of other competing metal ions. To further investigate the selectivity of **1a** for Cd^{2+} , we measured the absorption spectra of **1a** in the presence of Cd^{2+} mixed with various metal ions in HEPES-buffered solution (20 mM, $\text{CH}_3\text{CN}:\text{H}_2\text{O}$, 3:7, v/v, pH 7.0) (Figure 4). The absorbance of Cd^{2+} -bound **1a** is unperturbed in the presence of 10 equivalents of Na^+ , K^+ , Ba^{2+} , Ca^{2+} , Mg^{2+} , Cr^{3+} , Mn^{2+} , Fe^{3+} , Co^{2+} , Ni^{2+} , Cu^{2+} , Zn^{2+} , Pb^{2+} , Ag^+ , Al^{3+} , Cd^{2+} , Hg^{2+} , Hg^+ and Sn^{2+} , indicating excellent Cd^{2+} selectivity over these competing metal ions.

To further evaluate the responsive nature of **1a** toward Cd^{2+} , fluorescence titration was carried out with varying concentrations of Cd^{2+} in HEPES-buffered solution (20 mM, $\text{CH}_3\text{CN}:\text{H}_2\text{O}$, 3:7, v/v, pH 7.0). As shown in Figure 6 the chemosensor **1a** was almost non fluorescent, when 0–10 equivalents of Cd^{2+} was added to the solution of **1a** (10 μM), a gradual increase in fluorescence intensity at 495 nm was observed. The fluorescence intensity of the chemosensor **1a** at 495 nm was saturated when 10 equivalent Cd^{2+} were added. The absolute fluorescence quantum yield (ϕ_f) of **1a** goes from 0.10 to 0.88 upon Cd^{2+} binding. The spectral change indicates that a co-ordination linkage between **1a** and Cd^{2+} is formed and the **1a** could be a “turn on” fluorescence chemosensor for Cd^{2+} . As mentioned earlier also, selectivity of chemosensor **1a** toward other different metal ions (Na^+ , K^+ , Ba^{2+} , Ca^{2+} , Mg^{2+} , Cr^{3+} , Mn^{2+} , Fe^{3+} , Co^{2+} , Ni^{2+} , Cu^{2+} , Zn^{2+} , Pb^{2+} , Ag^+ , Al^{3+} , Hg^{2+} , Hg^+ and Sn^{2+}) was also investigated which displayed no changes in optical properties. Additionally, no significant fluorescence enhancement was observed upon addition of any other metal ion. Individual response of **1a** towards Cd^{2+} against these metal ions represents a remarkable selectivity only for Cd^{2+} binding (Figure 5). The Cd^{2+} -induced selective fluorescent enhancement of **1a** indicated that these response of the chemosensor may be attributed to the chelation enhanced fluorescence (CHEF) due to presence of chelating group such as C=O and –OH (Scheme 1). In addition, dilute solution of **1a** exhibited light blue fluorescence upon addition of Cd^{2+} and by irradiation with long UV light (Figure 1b).



Scheme 1: Proposed sensing mechanism of compound **1a** for Cd^{2+} .

Time resolved fluorescence studies of chemosensor **1a** in the absence and presence of Cd^{2+} ions have been done using an excitation wavelength of 387 nm in HEPES-buffered solution (20 mM, $\text{CH}_3\text{CN}:\text{H}_2\text{O}$, 3:7, v/v, pH 7.0). As shown in Figure 7b, the fluorescence lifetime increases from 0.217 ns to 1.97 ns after addition of Cd^{2+} ions indicating the strong complexation of **1a** with Cd^{2+} . These considerable changes in lifetimes of **1a**

ARTICLE

Journal Name

in the presence of Cd^{2+} proved its credentials as a good sensor for Cd^{2+} .

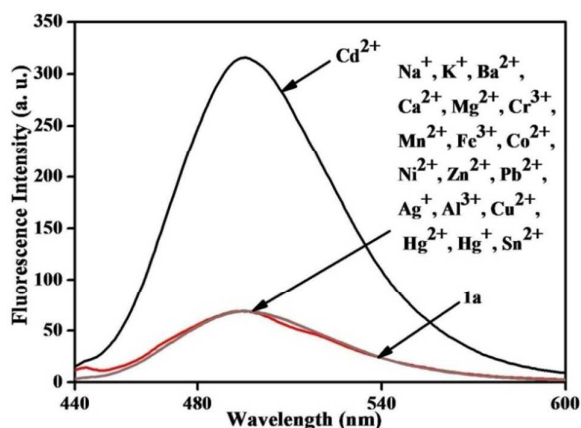


Figure 5: Fluorescence emission spectra of **1a** in the presence of different metal ions such as Na^+ , K^+ , Ba^{2+} , Ca^{2+} , Mg^{2+} , Cr^{3+} , Mn^{2+} , Fe^{3+} , Co^{2+} , Ni^{2+} , Cu^{2+} , Zn^{2+} , Pb^{2+} , Ag^+ , Al^{3+} , Cd^{2+} , Hg^{2+} , Hg^+ and Sn^{2+} in HEPES-buffered solution (20 mM, $\text{CH}_3\text{CN}:\text{H}_2\text{O}$, 3:7, v/v, pH 7.0). $\lambda_{\text{ex}} = 387$ nm, slit width = 3 nm.

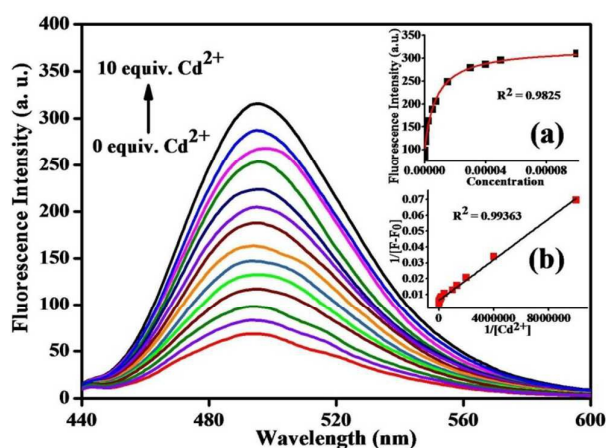


Figure 6: Fluorescence spectral response of **1a** (10 μM) upon titration with Cd^{2+} (0–10 equivalents) in HEPES-buffered solution (20 mM, $\text{CH}_3\text{CN}:\text{H}_2\text{O}$, 3:7, v/v, pH 7.0). Inset (a): Non linear fitting of fluorescence data of **1a** with Cd^{2+} . and Inset (b) A good linear fit of Benesi-Hildebrand plot confirms the 1:1 binding stoichiometry. $\lambda_{\text{ex}} = 387$ nm, slit width = 3 nm.

Moreover, the binding stoichiometry of **1a**- Cd^{2+} complex was revealed by Job's plot experiment. The fluorescence intensity at 495 nm was plotted as a function of the mole fraction of **1a** under a constant total concentration. The Job's plot approached the maxima when the molar fraction was 0.5, suggesting 1:1 binding stoichiometry ratio of **1a**- Cd^{2+} complex (Figure 7a). Furthermore, the binding constant was calculated to be $9.56 \times 10^5 \text{ M}^{-1}$ according to the Benesi-Hildebrand plot which also supports 1:1 binding stoichiometry of the complex **1a**- Cd^{2+} (Inset (b) of Figure 6). The binding constant was also evaluated by nonlinear least square fit,^{45, 46} which resulted a better binding constant $(1.34 \pm 0.87) \times 10^6 \text{ M}^{-1}$ (Inset (a) of

Figure 6) than the linear one. Non linear fitting indicated the 1:1 binding stoichiometry ratio of **1a**- Cd^{2+} complex.

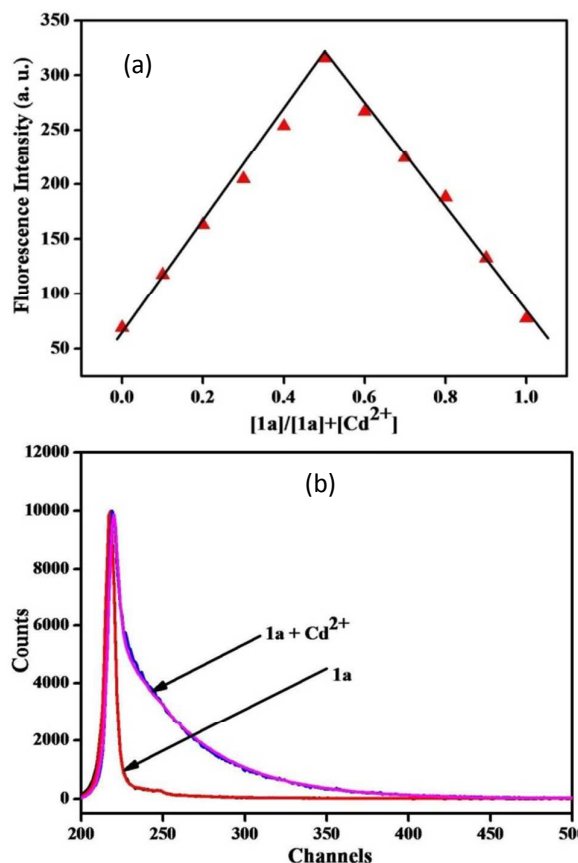


Figure 7: (a) Job's plot of **1a** and Cd^{2+} showing 1:1 stoichiometry of the complex **1a**- Cd^{2+} . (b) Fluorescence decay profile of **1a** in the absence and presence of Cd^{2+} (10 equiv.) in HEPES-buffered solution (20 mM, $\text{CH}_3\text{CN}:\text{H}_2\text{O}$, 3:7, v/v, pH 7.0). $\lambda_{\text{ex}} = 387$ nm, slit width = 3 nm.

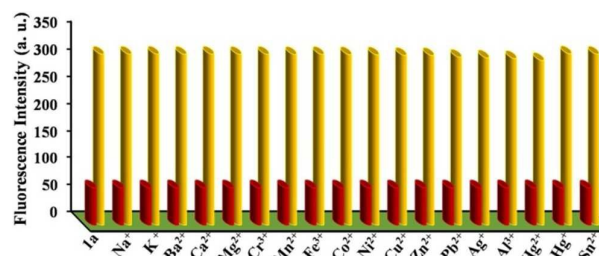


Figure 8: Metal-ion selectivity profiles of **1a** (10 μM) in HEPES-buffered solution (20 mM, $\text{CH}_3\text{CN}:\text{H}_2\text{O}$, 3:7, v/v, pH 7.0). Red bars represent the fluorescence intensity responses of **1a** in the presence of 10 equivalents of various metal ions. Yellow bars represent the fluorescence intensity responses of **1a**- Cd^{2+} complex in the presence of 10 equivalents of the indicated metal ions. $\lambda_{\text{ex}} = 387$ nm, slit width = 3 nm.

Selectivity of the sensor is very essential as the interference of other metal ions can affect its sensitivity and selectivity. In order to check the interference of the other metal ions, the

competitive binding studies of chemosensor **1a** were also performed. For the competitive binding experiment, equal concentrations of Cd^{2+} and other metals were taken. Among all the served metal ions no metal ion interferes were observed with the selectivity Cd^{2+} (Figure 8). Hence, chemosensor **1a** acts as an excellent sensor for Cd^{2+} even in the presence of other competition metal ions.

The limit of detection (LOD) was also determined from the fluorescence titration figures based on a reported method. According to the results of titration experiments, the fluorescence data were normalized between the minimum and the maximum value leading to the construction of a linear curve. The point at which this linear curve crossed the X-axis was considered as the detection limit. The detection limit was found to be 5.84×10^{-8} M (Figure S9 in the supporting information). The limit of detection (LOD) of the synthesized chemosensor **1a** was compared with some of the previously reported chemosensors for the determination of Cd^{2+} . It can be seen from the compared data in the supporting information Table 1S, the LOD of proposed sensor is significantly improved to the previously reported chemosensors for the determination of Cd^{2+} . We believe that chemosensor **1a** imparted sufficient sensitivity for the detection of a trace amount of Cd^{2+} in environmental samples.

The effect of pH on the emission response of **1a** in absence and presence of Cd^{2+} were measured and the results are shown in Figure 9. The fluorescence emission of chemosensor **1a** does not show any significant change over a wide pH range of 2 to 12. The chemosensor **1a** with Cd^{2+} displayed different fluorescence properties with emission band at 495 nm in neutral and basic medium. However, the fluorescence emission of **1a**- Cd^{2+} complex increases radically in the pH range from 5 to 7 and decreases in basic medium due to the formation of metal hydroxide.

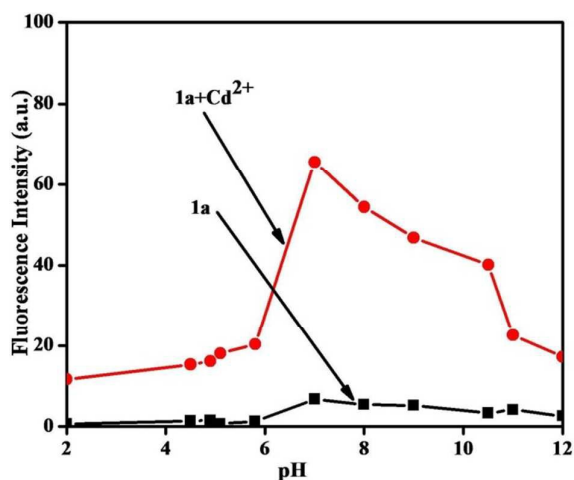


Figure 9: Fluorescence emission behavior of **1a** (black line) and **1a** + Cd^{2+} (red line) at different pH values.

The chemosensor **1a** with Cd^{2+} displayed excellent fluorescence emission at 495 nm at pH 7.0. Thus, these results demonstrate that the response behavior of **1a**- Cd^{2+} complex is pH independent in medium condition (pH 7.0–9.0). From the view of response speed of chemosensor **1a** and **1a**- Cd^{2+} , the pH 7.0 was chosen as optimum experimental condition.

Nature of interaction between chemosensor **1a** and Cd^{2+} ions

To further support the coordination mode between **1a** and Cd^{2+} as proposed above, FTIR and ESI-HRMS spectroscopic techniques experiment were performed by KBr pellets and CH_3CN , respectively. In the chemosensor **1a**, carbonyl group (C=O) of the chalcone scaffold and lactone of the coumarin ring, and the hydroxyl group of the coumarin moiety show characteristic IR peaks at 1608, 1716 and 3440 cm^{-1} , respectively (Figure S5). Unfortunately, upon addition of Cd^{2+} , the IR peak corresponding to the C=O group of the lactone on the coumarin ring did not display a marked shift while the peak corresponding to the C=O group of the chalcone scaffold was shifted to 1575 cm^{-1} . Furthermore the peak corresponding to –OH group of coumarin ring completely disappeared.

Moreover, to further investigate the binding mode of interaction, the ^1H NMR spectra of chemosensor **1a** in absence and presence of Cd^{2+} ions were also recorded (Figure S10). In ^1H NMR spectra of chemosensor **1a**, hydroxyl proton peak appeared at 18.99 ppm. Upon addition of 10 equiv. Cd^{2+} ions to the solution of chemosensor **1a**, the most significant change was observed in peak corresponding to hydroxyl proton which completely disappeared due to complexation with Cd^{2+} ion. However, the peak corresponding to the methoxy proton displayed slightly downfield shift and the peaks in aromatic region were also shifted slightly downfield. However, due to the co-existence of both keto and enol forms together in equilibrium, the peaks shifting is not very clear. These IR and ^1H NMR data confirmed that the C=O group of the chalcone scaffold and –OH group of coumarin ring were involved in the Cd^{2+} coordination, whereas the C=O group of the lactone on the coumarin ring did not participate in the metal-binding process. Moreover, HRMS (ESI+) m/z for **1a** calcd. $\text{C}_{19}\text{H}_{14}\text{O}_5$ $[\text{M}+\text{Na}]^+$: 345.0739, found 345.0747 and for **1a**+ Cd^{2+} calcd. $\text{C}_{19}\text{H}_{13}\text{CdO}_5$ $[\text{M}+\text{Cd}^{2+}]^+$: 434.9786, found 434.9763, has suggested about a 1:1 complexation between **1a** and Cd^{2+} (ESI, Figure S6 and S11).

Application: Visual colour changes on test papers

To explore the practical appliance of chemosensor **1a**, test strips were prepared by immersing strips into a CH_3CN solution of **1a** ($1.0 \times 10^{-4}\text{ mol L}^{-1}$) followed by dried in air. The **1a** containing test strips were utilized to sense Cd^{2+} ions by immersing test strips in to the solutions of Cd^{2+} ions ($5.0 \times 10^{-4}\text{ mol L}^{-1}$) for 10 sec and then the obvious colour change from yellow to colourless was observed (Figure 10). Thus, detection of Cd^{2+} could be easily carried by using these strips at any moment.

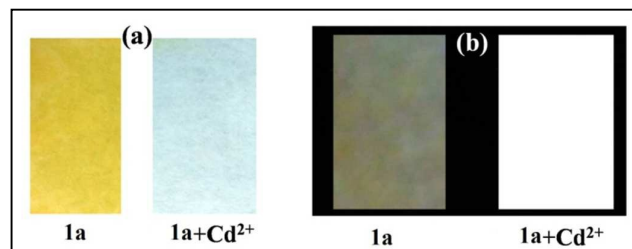


Figure 10: Photographs of (a) Colorimetric. (b) Fluorometric test kit: filter paper coated with **1a** (0.1 mM) for detecting Cd^{2+} in HEPES-buffered solution (20 mM, CH_3CN : H_2O , 3:7, v/v, pH 7.0).

Application of the proposed turn-on sensor to real samples

To explore the reliability and analytical applicability of the chemosensor **1a**, it was applied for determination of cadmium in three real samples lipstick, brown hair coloring material and the liquid foundation makeup cream. One gram of tiny pieces of lipsticks were dissolved in 8.0 mL of 65% HNO_3 and 2.0 mL of acetone. After 24 h, it was filtered, separated from the solid and dried. The dried material was dissolved in absolute ethanol and stirred at 1500 rpm for 2 h for complete dissolution of Cd^{2+} . After complete removal of solid material by centrifugation, the resulting solution was assayed for Cd^{2+} by the chemosensor **1a** and AAS. The same procedure was repeated for the brown hair coloring material and the liquid foundation makeup cream. The accuracy of the method has been verified by the determination of cadmium in all the samples by AAS (Table 1). The results obtained from these two methods (i.e. spectrofluorometry and AAS) proved that the synthesized chemosensor **1a** is highly selective and sensitive sensor for the monitoring of Cd^{2+} in different cosmetic and personal care samples.

Table 1: Determination of Cd^{2+} in cosmetic, and personal care samples by proposed fluorometric and AAS methods.

Real sample	Amount of Cd^{2+} (mol L^{-1})	
	Fluorometric	AAS
Lipstick	2.07×10^{-6}	1.96×10^{-6}
Hair Color	1.12×10^{-6}	1.06×10^{-6}
Makeup Cream	7.92×10^{-5}	7.20×10^{-5}

Experimental

All common reagents and solvents were used of AR grade. Metal salts used were obtained from HiMedia (Mumbai, India) and Loba Chemie (Mumbai, India). Spectroscopic-grade acetonitrile and water were used for electronic spectral and fluorescence studies. ^1H and ^{13}C nuclear magnetic resonance (NMR) spectra of compounds were recorded in CDCl_3 on a JEOL ECX-400-II spectrometer and chemical shifts are reported as part per million (ppm) in δ scale downfield from tetramethylsilane (TMS; as internal standard). The following

abbreviations are used to identify the multiplicities of the reported peaks: br, broad; s, singlet; d, doublet; dd, doublet of doublet; dt, doublet of triplet; t, triplet; q, quartet; m, multiplet. High-resolution mass spectrometry (HRMS) was performed on a Brüker microToF-Q-II electrospray-ionization (ESI) mass spectrometer. UV-vis. absorption spectra were recorded on a Shimadzu UV-2450 spectrophotometer and the fluorescence spectra were recorded on a Fluoromax-4 Spectrofluorometer with a 3-cm standard quartz cell. A Varian Atomic Absorption Spectrophotometer, (Model AA-240), was used for determination of Cd^{2+} . The pH was measured by means of an MRFS Toshniwal pH meter. Melting points were recorded on Optimelt automated melting point system. Quantum yield were obtained using FLS 980 fluorescence spectrometer (Edinburgh Instruments). IR spectra were recorded on an Alpha FTIR spectrometer (Bruker) in the range $4000\text{--}400\text{ cm}^{-1}$ with KBr pellets. Fluorescence life time spectra were obtained by using Horiba Jobin Yvon, Fluorocube fluorescence lifetime system.

UV-vis and Fluorescence measurements

Since the chemosensor **1a** was not completely soluble in 100% aqueous media, acetonitrile was used as a co-solvent. A stock solution of **1a** (1 mM) was prepared in acetonitrile and then sample solution of **1a** (10 μM) was prepared in phosphate buffered solution (20 mM, CH_3CN : H_2O , 3:7, v/v, pH 7.0), in a quartz cuvette (1 cm \times 1 cm). To the solution was added of 10 μL of an aqueous stock solution (10 mM) of metal salt (Na^+ , K^+ , Ba^{2+} , Ca^{2+} , Mg^{2+} , Cr^{3+} , Mn^{2+} , Fe^{3+} , Co^{2+} , Ni^{2+} , Cu^{2+} , Zn^{2+} , Pb^{2+} , Ag^+ , Al^{3+} , Cd^{2+} , Hg^{2+} , Hg^+ and Sn^{2+}). All fluorescence measurements of **1a** were carried out with slit widths of 3 nm.

Synthesis and characterization of (E)-4-hydroxy-3-(3-(4-methoxyphenyl)acryloyl)-2H-chromen-2-one, **1a**

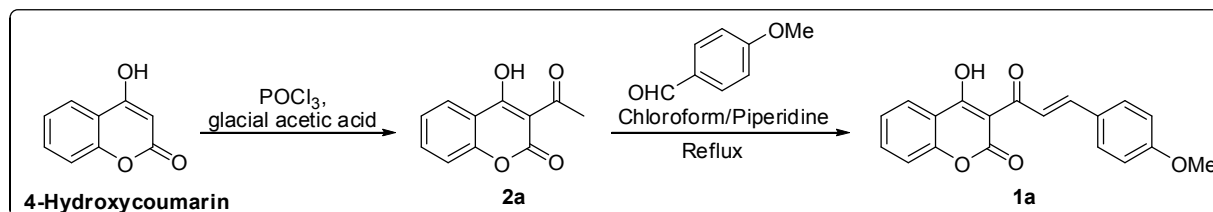
The two step synthesis of our target molecule started with the acetylation of commercially available 4-hydroxycoumarin in the presence of POCl_3 using glacial acetic acid as acetylating agent to furnish 3-acetyl-4-hydroxycoumarin, **2a**. Then the final step involved the condensation reaction between **2a** with 4-methoxybenzaldehyde in the presence of piperidine as a promoter in chloroform for 1.5 h to obtain the product **1a** (Scheme 2).

Step 1: Synthesis of 3-acetyl-4-hydroxy-2H-chromen-2-one, **2a**

To a solution of 4-hydroxycoumarin (162.14 mg, 1.0 mmol) in acetic acid (8.6 ml) was added phosphorus oxychloride (3.0 ml). The mixture was heated at reflux for 30 min. After cooling, the precipitate was collected and recrystallized from ethanol to give 3-acetyl-4-hydroxy-2H-chromen-2-one, **2a** as white needles (200.09 mg, 89 %). M.P = 135 $^\circ\text{C}$; $^1\text{H-NMR}$ (400 MHz, CDCl_3 , ppm): δ 2.79 (s, 3H), 7.28–7.37 (m, 2H), 7.69 (dt, J = 1.6, 7.2 Hz, 1H), 8.07 (dd, J = 6.4, 8.0 Hz, 1H); $^{13}\text{C-NMR}$ (100 MHz, CDCl_3 , ppm): δ 30.3, 101.5, 115.3, 117.2, 124.6, 125.8, 136.3, 154.9, 160.2, 178.8, 206.2; IR; ν_{max} (cm^{-1}) 3337, 2974, 2877, 2570, 1686, 1590, 1514, 1460, 1408, 1344, 1244, 1186, 1124,

Journal Name

ARTICLE

Scheme 2: Synthetic route of the chemosensor **1a**.

1072, 799, 741, 637. HRMS (ESI+) m/z for **1a** calcd. $C_{11}H_8O_4$ $[M+Na]^+$: 227.0320 found 227.0930.

Step 2: Synthesis of (E)-4-hydroxy-3-(3-(4-methoxyphenyl)acryloyl)-2H-chromen-2-one, **1a**

3-Acetyl-4-hydroxy-2H-chromen-2-one (204.17 mg, 1.0 mmol) and the appropriate substituted aromatic aldehyde (136.15 mg, 1.0 mmol) were dissolved in chloroform (1.0 mL). A catalytic amount of piperidine (0.66 mmol) was added and the reaction mixture was refluxed for 1.5 h. The chloroform was distilled out and the residue was washed with methanol and **1a** was obtained as a yellow solid (239.26 mg, 72 %). M.P = 136 °C; 1H -NMR (400 MHz, $CDCl_3$, ppm): δ 3.85 (s, 3H), 6.93 (d, J = 8.0 Hz, 2H), 7.27–7.33 (m, 2H), 7.64–7.68 (m, 3H), 8.02–8.08 (m, 2H), 8.31 (d, J = 16.0 Hz, 1H), 18.99 (s, 1H); ^{13}C -NMR (100 MHz, $CDCl_3$, ppm): δ 55.5, 100.5, 114.5, 114.6, 117.0, 119.9, 124.3, 125.8, 127.6, 131.5, 135.8, 147.5, 154.6, 162.6, 181.7; IR; ν_{max} (cm^{-1}) 3440, 2946, 2834, 1716, 1608, 1501, 1431, 1321, 1259, 1230, 1165, 1102, 1021, 994, 897, 822, 755, 667, 521. HRMS (ESI+) m/z for **1a** calcd. $C_{19}H_{14}O_5$ $[M+Na]^+$: 345.0739 found 345.0747.

Conclusions

We have successfully developed a coumarin–chalcone conjugate fluorescent sensor **1a** for the detection of Cd^{2+} over other competitive metal ions, e.g. Na^+ , K^+ , Ba^{2+} , Ca^{2+} , Mg^{2+} , Cr^{3+} , Mn^{2+} , Fe^{3+} , Co^{2+} , Ni^{2+} , Zn^{2+} , Pb^{2+} , Ag^+ , Al^{3+} , Cu^{2+} , Hg^{2+} , Hg^+ and Sn^{2+} . The chemosensor works as both a colorimetric and turn-on fluorescence probe for Cd^{2+} . It has the capability to detect Cd^{2+} in the nano-molar range with detection limits of 58.4 nM. The chemosensor behaves as a naked-eye and optical sensor for the determination of Cd^{2+} , with significant color changes on filter paper strips. The optimal pH for Cd^{2+} ions detection by chemosensor **1a** was 7.0 in HEPES-buffered solution (20 mM, $CH_3CN:H_2O$, 3:7, v/v). Thus, the coumarin–chalcone hybrid **1a** unambiguously demonstrates the function of Cd^{2+} detection in both solid states and solution with very

low detection limits. The practical ability of chemosensor **1a** was tested for the detection of cadmium ions in different cosmetic products with complex matrices and the results were obtained satisfactorily.

Acknowledgements

We thank Ministry of Human Resource and Development (MHRD), New Delhi, India [grant number MHR01-23-200-428], for financial supports.

Notes and references

- Z. Wang, M. A. Palacios and P. Anzenbacher, *Anal. Chem.* 2008, **80**, 7451.
- B. A. Fowler, M. Nordberg, L. Friberg and G. Nordberg, G. Handbook on the Toxicology of Metals, 3rd ed.; Eds.; Academic Press: Boston, MA, 2007.
- The European Parliament and the Council of the European Union, Directive on the Restriction of the Use of Certain Hazardous Substances in Electrical and Electronic Equipment. **2002/95/EC**.
- W. de Vries, P. F. A. M. Römken and G. Schütze, *Rev. Environ. Contam. Toxicol.* 2007, **191**, 91.
- B. A. Makwana, D. J. Vyas, K. D. Bhatt, S. Darji and V. K. Jain, *Appl. Nanosci.* 2016, **6**, 555.
- A. E. Sahnoun, L. D. Case, S. A. Jackson and G. G. Schwartz, *Cancer Invest.* 2005, **23**, 256.
- B. Julin, A. Wolk, J. E. Johansson, S. O. Andersson, O. Andrén and A. Åkesson, *Brit. J. Cancer.* 2012, **107**, 895.
- M. J. Mench, *Agric. Ecosyst. Environ.* 1998, **67**, 175.
- T. Jennings, Cadmium environmental concerns. PVC handbook, Munich, Germany, Hanser Verlag, 2005.
- M. J. Ahmed, M. Salim and J. B. Acad, Second Annual Report on Carcinogens, Environmental Protection Agency, NTP 81–43, December 1981, pp. 73–80.
- WorldHealthOrganization, Avenue Appia20, 1211 Geneva 27, Switzerland, http://www.who.int/water_sanitation_health/dwq/chemicals/cadmium/en/.
- S. Satarug and M. R. Moore, *Environ. Health Perspect.* 2004, **112**, 1099.
- M. Mameli, M. C. Aragoni, M. Arca, C. Caltagirone, F. Demartin, G. Farruggia, G. D. Filippo, F. A. Devillanova, A. Garau, F. Isaia, V.

ARTICLE

Journal Name

- Lippolis, S. Murgia, L. Prodi, A. Pintus and N. A. Zaccheroni, *Chem. Eur. J.* 2010, **16**, 919.
- 14 Q. Zhao, R.-F. Li, S.-K. Xing, X.-M. Liu, T.-L. Hu and X.-H. Bu, *Inorg. Chem.* 2011, **50**, 10041.
- 15 A. P. S. Gonzales, M. A. Firmino, C. S. Nomura, F. R. P. Rocha, P. V. Oliveira and I. Gaubeur, *Anal. Chim. Acta.* 2009, **636**, 198.
- 16 J. P. Lafleur, R. Lam, H. M. Chan and E. D. Salin, *J. Anal. At. Spectrom.* 2005, **20**, 1315.
- 17 Z. Zhu, Z. Liu, H. Zheng and S. Hu, *J. Anal. At. Spectrom.* 2010, **25**, 697.
- 18 H. N. Kim, W. X. Ren, J. S. Kim and J. Yoon, *Chem. Soc. Rev.* 2012, **41**, 3210.
- 19 Z. X. Wang, Y.-X. Guo and S.-N. Ding, *Microchim Acta* 2015, **182**, 2223.
- 20 P. Sianglam, S. Kulchat, T. Tuntulani and W. Ngeontae, *Spectrochim. Acta, Part A* 2017, **183**, 408.
- 21 S. Park and H. J. Kim, *Sens. Actuators, B* 2012, **168**, 376.
- 22 Y. Lv, L. Wu, W. Shen, J. Wang, G. Xuan and X. Sun, *J. Porphyrins Phthalocyanines.* 2015, **19**, 1.
- 23 J. Yan, L. Fan, J. C. Qin, C. R. Li and Z. Y. A. Yang, *J. Fluoresc.* 2007, **9**, 33.
- 24 Q. Zhao, R. F. Li, S. K. Xing, X. M. Liu, T. L. Hu and X. H. A. Bu, *Inorg. Chem.* 2011, **50**, 10041.
- 25 R. Khani, E. Ghiamati, R. Boroujerdi, A. Rezaeifard and M. H. Zaryabi, *Spectrochim. Acta. Part A.* 2016, **163**, 120.
- 26 X. J. Jiang, M. Li, H. L. Lu, L. H. Xu, H. Xu, S. Q. Zang, M. S. Tang, H. W. Hou and T. C. W. A. Mak, *Inorg. Chem.* 2014, **53**, 12665.
- 27 X. Liu, N. Zhang, J. Zhou, T. Chang, C. Fang, D. Shangguan, *Analyst*, 2013, **138**, 901.
- 28 E. J. Song, J. Kang, G. R. You, G. J. Park, Y. Kim, S. J. Kim, C. Kim and R. G. Harrison, *Dalton Trans.* 2013, **42**, 15514.
- 29 Z. Shi, Q. Han, L. Yang, H. Yang, X. Tang, W. Dou, Z. Li, Y. Zhang, Y. Shao, L. Guan and W. Liu, *Chem. Eur. J.* 2015, **21**, 290.
- 30 W. Su, S. Yuan and E. Wang, *J. Fluoresc.* 2017, DOI 10.1007/s10895-017-2124-0.
- 31 A.-J. Wang, H. Guo, M. Zhang, D.-L. Zhou, R.-Z. Wang and J.-J. Feng, *Microchim Acta* 2013, **180**, 1051.
- 32 X. Zhou, P. Li, Z. Shi, X. Tang, C. Chen and W. Liu, *Inorg. Chem.* 2012, **51**, 9226.
- 33 S. Goswami, K. Aich, S. Das, A. K. Das, A. Manna and S. Halder, *Analyst* 2013, **138**, 1903.
- 34 S. B. Maity, S. Banerjee, K. Sunwoo, J. S. Kim and P. K. Bharadwaj, *Inorg. Chem.* 2015, **54**, 3929.
- 35 B. A. Makwana, D. J. Vyas, K. D. Bhatt, S. Darji and V. K. Jain, *Appl Nanosci.* 2016, **6**, 555.
- 36 W.-B. Huang, W. Gu, H.-X. Huang, J.-B. Wang, W.-X. Shen, Y.-Y. Lv and J. Shen, *Dyes Pigm.* 2017, DOI: 10.1016/j.dyepig.2017.05.001.
- 37 X. Liu, P. Wang, J. Fu, K. Yao, K. Xue and K. Xu, *J. Lumin.* 2017, **186**, 16.
- 38 Y. Ma, F. Wang, S. Kambam and X. Chen, *Sens. Actuators, B* 2013, **188**, 1116.
- 39 X. Chen, C. S. Lim, D. Lee, S. Lee, S. J. Park, H. M. Kim and J. Yoon, *Biosens. Bioelectron.* 2017, **91**, 770.
- 40 Shaily, A. Kumar and N. Ahmed, *Supramol. Chem.* 2017, **29**, 146.
- 41 Shaily, A. Kumar, S. Kumar and N. Ahmed, *RSC Adv.* 2016, **6**, 108105.
- 42 Shaily, A. Kumar and N. Ahmed, *Ind. Eng. Chem. Res.* 2017, **56**, 6358.
- 43 A. Senthilvelan, I. T. Ho, K. C. Chang, G. H. Lee, Y. H. Liu and W. S. Chung, *Chem. Eur. J.* 2009, **15**, 6152.
- 44 H. A. Benesi and J. H. Hildebrand, *J. Am. Chem. Soc.* 1949, **71**, 2703.
- 45 J. Bourson, J. Pouget and B. Valeur, *J. Phys. Chem.* 1993, **97**, 4552.
- 46 M. J. Li, B. Wai-Kin Chu, N. Zhu, V. Wing-Wah Yam, *Inorg. Chem.* 2007, **46**, 720.
- 47 M. Shortreed, R. Kopelman, M. Kuhn and B. Hoyland, *Anal. Chem.* 1996, **68**, 1414.
- 48 W. Lin, L. Yuan, Z. Cao, Y. Feng and L. Long, *Chem. Eur. J.* 2009, **15**, 5096.